Characterization of coral-associated microbial aggregates (CAMAs) within tissues of the coral *Acropora hyacinthus*

Naohisa Wada[1,2,7], Mizuki Ishimochi[2,3], Taeko Matsui[2], F. Joseph Pollock[4,7,8], Sen-Lin Tang[1], Tracy D. Ainsworth[5], Bette L. Willis[6,7], Nobuhiro Mano[2, †], David G. Bourne[6,7,9 †]

[1]Biodiversity Research Center, Academia Sinica, Nangang, Taipei, Taiwan
[2]Department of Marine Science and Resources, College of Bioresource Science, Nihon University, Fujisawa, Kanagawa, Japan
[3]Faculty of Science, University of the Ryukyus, Nishihara, Okinawa 903-0213, Japan
[4]The Nature Conservancy, Caribbean Division, Coral Gables, FL 33134
[5]School of Biological, Earth and Environmental Science, University of New South Wales, Sydney, NSW, Australia
[6]College of Science and Engineering, James Cook University, Townsville, QLD, Australia
[7]AIMS@JCU, Townsville, QLD, Australia
[8]The Pennsylvania State University, State College, PA, USA
[9]Australian Institute of Marine Science, Townsville, QLD, Australia

†Equal correspond authors
Dr. Nobuhiro Mano (mano.nobuhiro@nihon-u.ac.jp) Department of Marine Science and Resources, College of Bioresource Science, Nihon University, Fujisawa, Kanagawa, 252-0813 Japan. Phone +81 466 84 3357
Dr. David G. Bourne (david.bourne@jcu.edu.au) College of Science and Engineering, James Cook University, Townsville, QLD, 4811 Australia. Phone +61 7 47814790

Kew Words: Coral Microbiome, Coral Tissue, Bacterial Aggregates, Fluorescent *in situ* Hybridisation

Abstract

Bacterial diversity associated with corals has been studied extensively, however, localization of bacterial associations within the holobiont is still poorly resolved. Here we provide novel insight into the localization of coral-associated microbial aggregates (CAMAs) within tissues of the coral *Acropora hyacinthus* using histological and fluorescent *in situ* hybridization approaches. In total, 318 CAMAs were characterized and shown to be distributed extensively throughout coral tissues collected from five sites in Japan and Australia. Density of basophilic CAMAs was typically higher at inshore sites (20.13 per cm^2 at inshore sites in Okinawa, Japan; 5.43 per cm^2 at inner shelf sites in the northern Great Barrier Reef) than at offshore sites on the GBR (0 to 1.1 per cm^2). CAMAs were randomly distributed across the six coral tissue regions investigated. Within each CAMA, bacterial cells had similar morphological characteristics, but bacterial morphologies varied among CAMAs, with at least five distinct types identified. Identifying the location of microorganisms associated with the coral host is a prerequisite for understanding their contributions to fitness. Localization of tissue-specific communities housed within CAMAs is particularly important, as these communities are potentially important contributors to vital metabolic functions of the holobiont.

Introduction

Scleractinian corals associate with a broad consortia of microorganisms, including endosymbiont dinoflagellates (*Symbiodiniaceae*), protozoa, fungi, bacteria, archaea and viruses, which collectively are termed the coral holobiont [1–3]. The importance of symbiotic dinoflagellates in provisioning the coral host with essential nutrients through translocated photosynthates has been well established [e.g.,4], however the roles of other microorganisms within the holobiont are less well understood. Some of the functions attributed to coral-associated microbiota include supply of essential nutrients and vitamins through processes such as nitrogen fixation [5–8] and metabolizing dimethylsulfoniopropionate (DMSP) to produce biologically important byproducts like dimethylsulfide [9]. The coral microbiome is also likely important for directly facilitating disease resistance through production of antimicrobials [10,11] or indirectly through microhabitat colonization that excludes opportunistic organism [12,13].

Corals are considered simple metazoans, but despite their basal phylogenetic position, they nevertheless form complex three-dimensional structures. Anatomically, the coral polyp consists of an outer mucus layer, two cell layers containing endosymbiotic dinoflagellates (inner layer) and nematocysts (outer layer), an external calcium carbonate skeleton, and a gastrovascular system that includes the coelenteron and connecting channels [14]. Within all these microhabitat niches, bacteria can reside as either transient communities or established symbionts with putative functional roles that may be positive, neutral or negative to the coral holobiont [15]. A multitude of studies have reported on the diversity of the coral microbiome, in some cases finding conserved

microbial communities associated with some coral species, and in others finding shifting microbiomes that reflect varying geographic, temporal or health status patterns [16–20]. To understand the significance of coral microbiome associations, care must be exercised so that diversity patterns reflect the specific ecological niche that these communities inhabit, such as the surface mucus layer, tissue layers, and/or the skeleton [21–28]. Defining the locations of specific microorganisms is essential for elucidating the importance of their role within the holobiont. For example, mucus bacteria are more likely to have a loose association with the coral host, being sloughed off as the mucus is exuded from the corals [29]. Conversely tissue-associated microorganisms are potentially more integrated in shared metabolic pathways and may reside in specific associations with host coral as a consequence of potential host selection [5,20].

To date, few studies have precisely localized bacterial communities within coral tissues. Studies that have focused on localization often find that bacterial communities within coral cell layers (i.e. epidermal and gastrodermal layers) form aggregations termed coral-associated microbial aggregates (CAMAs) [30,31]. CAMAs were first reported as potential pathogens when observed within healthy tissues of Caribbean corals displaying signs of white band disease [32,33]. Further studies subsequently reported that CAMAs are widespread in tissues of healthy corals sampled from geographically dispersed areas [31,33,34]. To date, CAMAs have been reported from 5 species of corals in the Caribbean [32,33] and 24 species from the Indo-Pacific [31], although their frequency varies among coral genera, with the genera *Acropora*, *Porites*, and *Pocillopora* most commonly hosting bacterial aggregates [31]. Identification of the

microorganisms that constitute these CAMAs has been poorly resolved. Neave et al. (2016) visualized aggregates (i.e., "cyst-like aggregations") of *Endozoicomonas* within tissues of *Stylophora pistillata* at the interface of the epidermis and gastrodermis in samples taken from widely-separated biogeographic regions [35]. However, the fine-scale spatial distributions of microorganisms and potential microhabitat-associated structure of the microbiome still have not been clarified. Here, we visualize the localization, distribution and morphology of CAMAs associated with the coral *Acropora hyacinthus* sampled from Sesoko Island, Okinawa, Japan and sites in the northern Great Barrier Reef (GBR) Australia located along an inshore to offshore gradient.

Results

Comparison of CAMA abundance among geographic locations

At the time of field collection, all 48 colonies of *A. hyacinthus* sampled from the 5 geographic locations (see **Fig. 1**) appeared visually healthy. This was confirmed by subsequent histological analyses, which found that all tissues displayed normal cell morphology, including no signs of fragmentation, wound repair or necrosis (as per criteria in Work and Aeby 2011). In total, 318 CAMAs were characterized via histology within coral tissues from the 48 samples. The vast majority stained basophilic (95.9%) using the standard haemotoxylin and eosin stain, compared to only 4.1 % staining eosinophilic (**Fig. 2**). Of the 48 colonies collected across all five sites, CAMAs were detected in 27 of the colonies (~56%). At one site (Sesoko Island), tissues from all 10 colonies sampled contained CAMAs (**Fig. 2c**), whereas at the other four sites, CAMAs

were observed only in some of the coral tissues sampled. For example, clear CAMAs were visible in 80% of Inner Shelf samples, 30% of Lizard Island, 25% of Outer Shelf, and 40% of Orpheus Island samples (n=10 samples at all sites, except at the Outer Shelf site where n=8 samples) (**Fig. 2c**). In general, the abundance of CAMAs was significantly higher at the inshore Sesoko Island site than at more offshore sites (Lizard Island, Outer Shelf, and Orpheus Island sites; $p < 0.05$).

The density of basophilic CAMAs in tissues was significantly higher for the Sesoko Island and Inner Shelf sites compared to the other three sites, with 20.13±17.1 and 5.43±8.7 basophilic CAMAs detected per cm^2 of tissue at these two sites, respectively (**Fig. 2d**; $p < 0.05$). In one sample from Sesoko Island, 48.9 CAMAs were detected per cm^2 of tissue, the greatest density of CAMAs observed in the 48 samples investigated. This is in contrast to an average of 0.28±0.4, 0 and 1.1±2.3 CAMAs per cm^2 for the Lizard Island, Outer Shelf and Orpheus Island samples, respectively (**Fig. 2d**). In contrast, the abundance of eosinophilic CAMAs did not differ significantly among the five sites, although the density of CAMAs was higher at the Outer Shelf, GBR site (1.3±3.5 CAMAs per cm^2, **Fig. 2d**) than at other sites (Sesoko Island: 0 CAMAs per cm^2; Inner Shelf, GBR: 0.1±0.3 CAMAs per cm^2, Lizard Island, GBR: 0 CAMAs per cm^2; Orpheus Island, GBR 0.2±0.7 CAMAs per cm^2).

Distribution of CAMAs within anatomical regions of the coral polyp

Specific detection of bacteria by fluorescent *in situ* hybridization (FISH) can be problematic for coral samples due to nonspecific binding of probes and background

autoflorescence of granular cells and nematocysts [37]. Therefore, CAMAs were identified by their characteristic shapes, in addition to fluorescent signals derived from binding to the general bacteria-targeted probe set EUB338mix and comparisons to background autofluorescence and non-specific binding (using Non338 probe). A total of 307 CAMAs were identified and localized by FISH (170 in Sesoko Island samples, 126 in samples from Inner Shelf sites in the Northern GBR, 4 from Lizard Island, 2 from Outer Shelf sites in the Northern GBR, and 5 from Orpheus Island samples). CAMAs were found within six anatomical regions of the coral polyp: the tentacle, actinopharynx, mesentery, mesenterial filament, coenosarc and calicoblastic layer (see **Fig. 3a**). Thirty-one additional CAMA-like shaped structures were observed (from three samples derived from Sesoko Island), but these were discounted as bacterial aggregates due to non-probe binding signals and excluded from further downstream analysis. The CAMAs appeared to be randomly distributed across the anatomical regions investigated, although because the numbers of CAMAs characterized for the Lizard Island, Outer Shelf and Orpheus Island samples were low (**Fig. 3b**), meaningful comparisons can only be made between the Sesoko Island and Northern Inner Shelf samples. For the Sesoko Island samples, CAMAs were found predominantly in the tentacles (36.5%), mesenterial filaments (34.7%) and coenosarc (16.5%) regions; in Inner Shelf samples from Northern GBR sites, CAMAs were mostly located in the calicoblastic layer (46.8%), tentacles (17.5%) and coenosarc (16.7%) (**Fig. 3b**).

CAMAs spanned a wide size range, from 23 to 6,761 μm^2 across tissue samples from all sites (**Fig. 3c**). In general, measurements underestimated the size of

CAMAs, given that measurements were dependent on the orientation of sectioning and it is unlikely that most CAMAs were sectioned through their greatest diameter. Acknowledging constraints associated with sectioning, the average size of CAMA's was 1,304 μm^2. On average, Sesoko Island samples contained larger aggregates (1,507.7±1,522.4 μm^2) than samples from the GBR region (Inner Shelf: 637.4±734 μm^2. However, given the large range in sizes measured, the fact that only two locations had sufficient sample sizes for comparison, and the issue of sectioning orientation potentially biasing size measurements, such patterns require further validation. No patterns in the size of CAMAs across different anatomical regions were detected (**Fig. 3c**).

Morphology of CAMAs within coral tissues

High resolution imaging was used to partially characterize and compare the morphology of bacteria across the CAMAs detected (**Fig. 4**). Interestingly, each CAMA appeared to be composed of a single morphological type of bacteria, although morphological types varied among CAMAs. Overall, five different morphological types of bacteria were identified: rod-shaped (length 2.5±0.1 µm, width 0.6±0.0 µm, **Fig. 4a, e**), an atypical cocci (length 4.8±0.3 µm, width 3.1±0.2 µm, **Fig. 4b, f**), a longer rod morphology (length 8.0±0.0 µm, width 0.8±0.0 µm, **Fig. 4c, g**), filamentous-like bacteria (length N.D., width 0.4±0.0 µm, **Fig. 4d, h**), and a rod-shaped morphology but with spore-like structures (**Fig. 4i–j**, **m–n**). While the consistency of morphological characteristics within each CAMA may indicate that CAMAs are hosting single

bacterial types, it is also possible that they host multiple bacterial species with similar morphologies. Interestingly, the fluorescent signal detected for some CAMAs was not uniform over the entire aggregation. The lack of signal within some CAMAs (see **Fig. 4d** for example) may be due to the probe not targeting microbial cells that inhabit that space. Defining a specific morphological shape for the bacterial cells observed was sometimes difficult, with patchy probe hybridization producing images of structures that potentially protruded from the tissue sections and seemed amorphous (**Fig. 4k–l, o–p**). However, this again could be the result of mixed microbial communities within the CAMA's, with some cells targeted by the probes, but others not hybridizing to the probe-fluorochrome conjugate.

Further three-dimensional reconstructions of z-stacked FISH images of select 100 µm stained sections of tentacles visualized the CAMAs as typically spheroid or ellipsoid-shaped structures (**Fig. 5a**). In one example, a single CAMA was located independently in the ectoderm of a tentacle (**Fig. 5b**). In a different tentacle, multiple smaller CAMAs were localized close to *Symbiodiniaceae* cells in the gastrodermal region (**Fig. 5c**). Sizes of the large single CAMA and the multiple smaller CAMAs were 33,400 μm^3 (**Fig. 5d**, surface area 7,729 μm^2) and 1,978 ± 141.2 μm^3 (**Fig. 5e**, 809.5 ± 59.9 μm^2, n=4 CAMAs), respectively. Even though the CAMAs were located in the same polyp, the size of the single large CAMA was approximately 40-fold greater than the multiple smaller CAMAs, demonstrating inherent size variability for these structures. The bacteria within these CAMAs displayed a similar rod-shaped morphology (see **Fig. 4a and e**), with the average cross-sectional area of each bacterium being 175.7 μm^2 and

22.6±4.2 μm^2, respectively (**Suppl. Fig. 2**). Based on cell size, the number of individual rod-shaped bacterial cells within the 3D rendered images of these CAMAs was estimated as ~ 47,275 cells for the large single CAMA located in the ectoderm of the tentacle (**Fig. 5d** and **Suppl. Fig. 2a**), and 2,799±200 cells (**Fig. 5e** and **Suppl. Fig. 2b**) for each of the smaller CAMAs localized close to *Symbiodiniaceae* cells.

Discussion

The importance of microbial symbionts to their hosts has been demonstrated for many animals, through acquisition and passage of nutrients, niche space occupation and shared metabolic pathways [38–40]. For corals, the fundamental roles that endosymbiotic dinoflagellates (*Symbiodiniumecae*) play in fitness of the coral holobiont have long been established [e.g., 41,42], but although many studies have postulated the importance of bacterial communities to coral fitness (see in the review) [3], direct evidence is still mostly lacking [15]. To facilitate a more comprehensive understanding of the roles bacterial communities may play in the coral holobiont, an improved understanding of the localization of these microbial communities is essential, particularly tissue-associated bacterial communities housed within structures termed coral-associated microbial aggregates (CAMAs). In this study, we provide high resolution characterization of these aggregations in tissues of *A. hyacinthus* sampled from sites in Japan and the Great Barrier Reef, Australia, including estimates of CAMA distributions, density and size, as well as visualization of the morphologies of bacterial cells within these structures.

We found that CAMAs commonly occur in healthy tissues of the coral *Acropora hyacinthus* collected from sites in Japan and Australia separated by more than 40 degrees of latitude. Although CAMAs were not detected in all tissue samples collected, this may reflect limitations in the area of coral tissue that can be surveyed via histological approaches. The presence of CAMAs in a histological section will depend on the tissue sectioned (i.e. the location of the fragment on the colony and on the section from the fragment), and on the scale and orientation of the section. Therefore, although not all coral tissue samples (and therefore not all colonies) were found to host CAMAs, we cannot exclude the possibility that other tissue areas of the same colony had CAMAs present. Other studies have also reported that CAMAs are common in tissues of many coral species in the Caribbean [32,33], Indo-Pacific and Red Sea [31,34,35]. In particular, CAMAs were common in species of *Acropora*, *Porites*, and *Pocillopora*, although often their presence was patchy within a population sample [31].

Interestingly, CAMAs were detected in a higher proportion of samples from inshore sites (i.e., 100% of Sesoko Island samples, 80% of samples from the northern GBR Inner Shelf site) than from offshore sites (25-40% of samples). Tissue density of CAMAs was also greatest in inshore samples (20.1±17.1 and 5.4±8.7 CAMAs per cm^2 for Sesoko Island and Inner Shelf GBR samples, respectively), and densities progressively decreased in tissues from the three more offshore sites (<1.2 CAMAs per cm^2), culminating in 0 CAMAs per cm^2 in the northern GBR Outer Shelf samples. Although our study provides only a snapshot of five sites sampled at one time point, it suggests that inshore reef environments may promote the development of CAMAs

within coral tissues. The inshore site at Sesoko Island has high nutrient influxes, especially phosphates [43,44]. Similarly, nearshore GBR sites are influenced by influxes of dissolved nutrients from terrestrial runoff, with higher concentrations typically found at inshore compared with offshore sites [45]. Temperature fluctuations may also influence CAMA abundance, although differences in seasonal temperature fluctuations are minimal across the northern GBR sites [46]. The coral microbiome community has been shown to shift in response to environmental stressors [29,47–52], thus water quality parameters influencing microbiological composition and function [53] could stimulate CAMA abundance. Further studies, particularly of potential links between nutrient levels and CAMA development, are needed to understand what might drive the increased prevalence and density of CAMAs in coral tissues at inshore sites, and to determine if hosting more CAMAs is beneficial to corals or is an indicator of negative impacts on the coral holobiont.

Localization of CAMAs using FISH demonstrated that they occur in all six of the anatomical regions investigated, i.e., the tentacle, actinopharynx, mesentery, mesenterial filament, coenosarc and the calicoblastic layer. CAMAs were highly variable in size, spanning a range from 23 to 6,761 μm^2 in area, with no obvious pattern in size when analyzed by anatomical region or geographic site. Although Sesoko Island samples contained larger aggregates on average (average cross-sectional area of 1,507.7±1,522.4 μm^2) than other sampling sites, low numbers of CAMAs in tissues from some sites, combined with potential bias introduced by sectioning, limit the

conclusions that can be drawn. Nevertheless, investigation of the potential influence of water quality parameters on the size of CAMAs is warranted.

Estimating the number of cells within CAMAs using 3D imaging revealed that a CAMA with a cross-sectional area of 22.6±4.2 μm^2 would be composed of ~2,800 rod-shaped bacteria. Based on similar methods, we further extrapolated that bacterial densities in tissues from Sesoko Island and Inner Shelf GBR corals are approximately 5.6×10^4 and 1.5×10^4 cells per cm^2 (along a linear cross-section), respectively. Very few studies have accurately determined bacterial cell densities associated with corals. Counts for bacteria in the coral mucus layer can be as high as 10^7 cells ml^{-1} [54]. Estimates of bacteria on tissue surfaces range from 1×10^5 to 10^6 cells per cm^2 for the coral *Pocillopora damicornis* [55] and 8.3×10^6 to 6.2×10^7 cells per cm^2 for the coral *Oculina patagonica* [24]. However, these counts are based on bacteria external to coral tissues and therefore not directly comparable to estimates from our 3D reconstructions of CAMAs visualized within coral tissues. Our results highlight that tissue-associated communities exist and that differentiating these communities from external and mucus-associated microbial communities is important for accurate appraisals of the coral microbiome and for identifying their role(s) within the coral holobiont.

An important finding from our high-resolution FISH imaging study is that in most cases, each CAMA contained bacterial cells that were consistent in their morphological appearance. Moreover, bacterial morphologies varied among CAMAs, with up to five different cell morphologies detected. This variation in bacterial cell

morphology among CAMAs may explain why the histological staining properties of CAMAs varied, the majority being basophilic (95.9%), but 4.1% staining eosinophilic (n=318 CAMAs detected in total). Similar variability in the staining of CAMAs has been reported previously [31,56], and has been attributed to varying degrees of protein and DNA production or local tissue pH conditions [31]. However, our finding that different morphological variants of bacteria are housed within different CAMA's potentially contributes to variation in the H&E staining observed. Previous studies have reported that the abundant coral-associated bacterial genera *Endozoicomonas* forms aggregates within tissues of the corals *Stylophora pistillata* and *Pocillopora verrucosa* [35,57]. Indeed, extensive sequence-based phylogenetic surveys of coral microbiomes have revealed that several dominant bacterial groups are common [20], including the *Proteobacteria* (particularly *Alpha*- and *Gamma-proteobacteria* inclusive of *Endozoicomonas*), as well as *Actinobacteria*, *Bacteroidetes* (especially *Flavobacteria*), and *Cyanobacteria* [3]. Hence some of the different cellular morphologies we detected within CAMAs may represent common coral-associated bacterial groups profiled in microbiome diversity studies. In addition, two dominant bacteria were found to be localized intercellularly within *Symbiodiniaceae* residing in the gastrodermal layers of coral host tissues using both sequencing and FISH [27]. We note, however, that bacterial morphology can be plastic and dependent on numerous variables, such as division stage, colonization, chemical environment, physical constraints and nutrient availability [58]. Future work targeting CAMAs with taxa-specific probes and gene sequencing approaches would

help to resolve both the taxonomy and potential functional roles of bacterial types within the holobiont.

FISH imaging showed that, for some of the CAMAs, patchy probe-specific labeling occurred, resulting in dull or dark areas within the structures. There are a number of potential methodological reasons for this observation, including: 1) insufficient probe sensitivity due to low ribosomal rRNA content in target cells [59,60], 2) methodological and environmental factors that prevent probes from accessing target cellular rRNA at these sites [61], 3) the bacterial community penetrating and proliferating within the outer epidermal layer of coral tissues [34], or 4) lipid or fat solvents deposited through dehydration and dewaxing steps showing empty spaces in the tissues [62]. Alternatively, little to no signal in central regions of some of the CAMAs could indicate that the probe EUB338mix did not target the taxonomic group of microbes within these regions. The EUB338mix is estimated to cover 96% of the *Eubacteria* domain, but taxa outside this coverage, including archaeal lineages, may be present [63]. We speculate that some of the CAMAs may be mixed communities containing bacteria not targeted by the probes or even *Archaea*, which have been identified to associate with corals in microbiome diversity studies [64]. A recent coral metagenomic study recovered *Thermarchaeota* genome bins from a *Porites sp* that was potentially metabolically linked through nitrogen cycling to other coral microbial-associated taxa, including *Nitrospira* [5]. Co-aggregation of ammonia-oxidizing archaea with nitrite-oxidizing bacteria is common in other organisms, such as sponges [65,66]. Findings that CAMAs are often co-localized near *Symbiodiniaceae* cells highlights the need for further isotope

studies to visualize and validate potential metabolic integrated links between bacterial, archaeal and *Symbiodiniaceae* symbionts.

Conclusion

Localization of microorganisms associated with corals is vital to understand their symbiotic relationships and reveal their function(s) within the holobiont. Here we provide novel insight into the distributions and densities of bacteria within tissues of the coral *Acropora hyacinthus* sampled from five different locations. CAMAs were common in coral tissues sampled, although their abundance differed across geographic sites. While each CAMA appeared to be dominated by a single bacterial morphological type, different CAMA hosted different bacterial morphotypes. CAMAs have been defined as facultative symbionts, not necessary for host fitness [31], however their high prevalence and abundance in coral tissues may indicate they are integrated into shared metabolic pathways and central to maintaining coral fitness through provisioning benefits. Such propositions require testing by tracing metabolic pathways, as well as improved taxonomic and functional assessment of the microorganisms housed within these CAMAs.

Materials and methods (less than 1500 words)

Fragments (~ 3 cm x 3 cm; n=48 colonies) of the tabulate coral *Acropora hyacinthus* (Dana, 1846) were collected from five geographic locations across two countries (Australia and Japan). Samples from Japan (n=10) were collected from

Sesoko Island (26˚37'40.3"N, 127˚51'36.4"E, depth 1.5–3.0 m, colony size 62.8±41.7 cm) in Okinawa, Japan in July 2015. On the Great Barrier Reef (GBR) Australia, samples were collected from the Northern sector along an inshore to offshore gradient inclusive of Lizard Island (see Fig. 1; n=10 from an Inner Shelf site (14˚47’29.4”S, 145˚20’18.8”E, depth 3–5 m, colony size 77.69±43.0 cm), n=10 from Lizard Island (14˚68’60.40”S, 145˚44’49.56”E, depth 2–4 m, colony size 61.67±17.5 cm) and n=8 from an Outer Shelf site (14˚38’30.0”S, 145˚38’22.5”E, depth 2–5 m, 41±20.5 cm)) in February 2012. Samples (n =10) were also collected from reefs around Orpheus Island (18˚35’55.4”S, 146˚29’33.8”E, depth 2–3 m, colony size N.D.) in the inner central region of the Great Barrier Reef in March 2012.

Following collection, samples were immediately rinsed with sterile seawater and then fixed in 4% paraformaldehyde (Electron Microscopy, USA and Wako, Japan) in 10mM phosphate buffered saline (PBS; pH 7.4) for 8–10 hours maintained at 4 ˚C. Samples were subsequently rinsed twice with 70% ethanol and stored in 70% ethanol at 4 ˚C prior to decalcification. After samples were rinsed by PBS twice for 30 min each, samples were decalcified at 4 ˚C in a 10% EDTA (sigma-Aldrich, USA) solution (w/v; pH 8.0 adjusted by sodium hydroxide [Wako, Japan]), which was exchanged approximately every two days until no coral skeleton remained. The decalcified samples were rinsed in PBS, and dehydrated sequentially through 70%, 90%, abs. 100% and abs. 100% ethanol series (60 min each), then processed through a 1:1 solution of abs. 100% ethanol and toluene and two toluene (30 min each), and embedded in paraffin. Nine sections (three serial sections x three sets; interval = 100 µm between each set) of each

coral fragment, each 4 µm thick, were cut from each paraffin-embedded sample (Suppl. Fig. 3). In addition, thicker 100 µm sections were cut from coral tissues to allow reconstructions of three-dimensional configurations of the CAMAs (see below). Serial sections were mounted on one slide coated with egg-white glycerin and on two slides with poly-L-lysine solution (Sigma-Aldrich, USA) for HE staining and fluorescence *in situ* hybridization (FISH), respectively. We analyzed a total 144 sets (432 sections) of the serial sections for H&E staining and FISH among five location sites.

For HE staining, one serial section from each set was dewaxed in xylene (2 x 15 min), rehydrated through ethanol series with abs. 100%, 99%, 90% and 70% (5 min each) and rehydrated completely in sterile water. Hydrated sections were stained in Mayer's hematoxylin (Wako, Japan) for 10 min, rinsed in water for 5 min, then stained with eosin Y (Merck, Germany) for 5 min, and further rinsed in water for 30 sec. The stained sections were dehydrated through the same ethanol series in reverse with agitation (few sec each), cleared by xylene (2 x 5 min) and finally mounted in Entellan mounting medium (Merck, Germany). HE stained sections were observed and recorded using an ECLIPSE Ni microscope (Nikon, Japan) and BIOREVO BZ–9000 microscope (KEYENCE, Japan).

The other two serial sections from each set were subjected to FISH according to the protocol detailed in Wada et al. (2016) [37]. Briefly, sections were dewaxed in xylene (2 x 15 min), dehydrated briefly once in 100% ethanol and dried completely. The dried sections were immersed in a 0.2 M HCl solution for 12 min, followed by a 20 mM Tris-HCl solution (pH 8.0) for 10 min at room temperature. The sections were

mounted with proteinase K (50 µg ml^{-1}) in 20 mM Tris-HCl solution at 37 ˚C for 5 min for bacterial cell wall permeabilization, and washed in a 20 mM Tris-HCl solution at room temperature for 10 min. Oligonucleotide probes, including a probe targeting the 16S rRNA gene (EUB338mix: 5'-GCWGCCWCCCGTAGGWGT-3') and a nonsense, negative control probe (Non338: 5'- ACATCCTACGGGAGGC -3'), were labeled with the Cy3 fluochrome (eurofins, USA) [67,68]. Tissue sections were covered with hybridization buffer (30% v/v formamide, 0.9 M NaCl, 20 mM Tris-HCl [pH 8.0], 0.01% SDS), then each oligonucleotide probe was added to a final concentration of 25 ng $µl^{-1}$ to each serial section. The slides were incubated at 46 ˚C for 1.5 hour. After incubation, sections were washed in 50 ml falcon tubes containing preheated wash buffer (0.112 M NaCl, 20 mM Tris HCl [pH 8.0], 0.01% SDS, 5 mM EDTA [pH 8.0]) in a water bath at 48 ˚C for 10 min, then soaked immediately with agitation in cold water, and air dried completely. The dried sections were mounted in an antifade mounting medium Fluoromount/Plus (Diagnostic BioSystems, USA). Sections were examined and recorded using a FV1000-D confocal microscope (Olympus, Japan) with two channels, using the following settings: (1) laser: 405 nm and 559 nm; (2) excitation dichroic mirror: DM405/473/559; (3) emission dichroic mirror: SDM560 and mirror; (4) band-pass filter: None and BA575–620 for detecting autofluorescence of coral tissue (blue) and Cy3 signal (red), respectively. Non-specific probe binding in tissue sections was identified as detailed by Wada et al. (2016)[37].

Three-dimensional images (3D) of CAMAs were reconstructed from the thick sections (100 µm) which were cut carefully from two samples (S6 from the Sesoko

Island and LO8 from the Outer Shelf GBR site). Sections were visualized via FISH according to methods described above, and examined using a LSM 880 (ZIESS, Germany) with two tracks and the following settings: (1) laser: 405 nm and 561 nm; (2) beam splitter: MBS -405 and MBS 488/561; (3) filter: 371–479 nm for auto-fluorescence of coral tissue (blue) and 627–758 nm for *Symbiodiniaceae* (green) in track 1 and 565–588 nm for Cy3 signals (red) in track 2, respectively. For reconstructing the 3D images, the sections consisted of z-stack images at 3.0 µm intervals for 10x and 0.7 µm each and 40x magnifications using the Z-stack function in LSM 880. The z-stack images were processed and reconstructed with surface rending of the Cy3 signals in Imaris software ver. 8.0.2 (BitplaneAG, USA).

Statistical analysis was conducted using R Stats ver. 3.5.1 [69] with the following packages: DescTools ver. 0.99.26 [70], dplyr ver. 0.7.6 [71], FSA ver. 0.8.20 [72], lattice ver. 0.20–36 [73], and rcompanion ver. 2.0.0 [74]. To compare the abundances of CAMAs at the colony level among sites, G-tests followed by post hoc Bonferroni corrections were used. To evaluate the density of CAMAs within coral tissues, we compared the distribution of CAMAs among five sites using the Kruskal-Wallis test with Dunn's multiple comparison followed by a Benjamini-Hochberg correction method.

Author contribution

NW, NM and DB conceived the study. NW, JP and DB designed the sampling and FISH experiments. NW and JP conducted the field sampling. NW, MI and TM

performed the histological work and all observations and data collection. NW and DB had major contribution in the manuscript writing and the figure making. JP, ST, TA, BW and NM contributed to writing and editing the manuscript. All authors critically reviewed, revised and ultimately approved this final version.

Acknowledgements

Dr. Joleah Lamb (Cornell University), Mr. Sefano Katz (Pacific Blue Foundation), Dr. Gergely Torda (ARC Center of Excellence for Coral Reef Studies, James Cook University), and Dr. Melanie Trapon (CSIRO) are thanked for helping to collect samples. We are also grateful to Mr. Yasuhiko Sato from Ziess Microscopy Japan, and Mr. Ji-Ying Huang and IPMB Live-Cell-Imaging Core Lab in the Institute Academia Sinica for supporting the microscopy and Imaris software used, respectively.

References

1. Rohwer, F., Seguritan, V., Azam, F. & Knowlton, N. Diversity and distribution of coral-associated bacteria. *Mar. Ecol. Prog. Ser.* **243**, 1–10 (2002).
2. Rosenberg, E., Koren, O., Reshef, L., Efrony, R. & Zilber-Rosenberg, I. The role of microorganisms in coral health, disease and evolution. *Nat. Rev. Microbiol.* **5**, 355–62 (2007).
3. Bourne, D. G., Morrow, K. M. & Webster, N. S. Insights into the Coral Microbiome: Underpinning the Health and Resilience of Reef Ecosystems. *Annu. Rev. Microbiol.* **70**, 317–340 (2016).
4. Yuyama, I., Ishikawa, M., Nozawa, M., Yoshida, M. & Ikeo, K. Transcriptomic changes with increasing algal symbiont reveal the detailed process underlying establishment of coral-algal symbiosis. *Sci. Rep.* **8**, 16802 (2018).

5. Robbins, S. J. *et al.* A genomic view of the coral holobiont. *Nat. Microbiol.* (in press).
6. Lema, K. A., Willis, B. L. & Bourne, D. G. Corals Form Characteristic Associations with Symbiotic Nitrogen-Fixing Bacteria. *Appl. Environ. Microbiol.* **78**, 3136–3144 (2012).
7. Pogoreutz, C. *et al.* Nitrogen Fixation Aligns with nifH Abundance and Expression in Two Coral Trophic Functional Groups. *Front. Microbiol.* **8**, (2017).
8. Yang, S.-H. *et al.* Metagenomic, phylogenetic, and functional characterization of predominant endolithic green sulfur bacteria in the coral Isopora palifera. *Microbiome* **7**, 3 (2019).
9. Raina, J.-B. *et al.* DMSP biosynthesis by an animal and its role in coral thermal stress response. *Nature* **502**, 677–680 (2013).
10. Raina, J.-B. *et al.* Isolation of an antimicrobial compound produced by bacteria associated with reef-building corals. *PeerJ* **4**, e2275 (2016).
11. Gochfeld, D. J. & Aeby, G. S. Antibacterial chemical defenses in Hawaiian corals provide possible protection from disease. *Mar. Ecol. Prog. Ser.* **362**, 119–128 (2008).
12. Ritchie, K. B. Regulation of microbial populations by coral surface mucus and mucus-associated bacteria. *Mar. Ecol. Prog. Ser.* **322**, 1–14 (2006).
13. Shnit-Orland, M. & Kushmaro, A. Coral mucus-associated bacteria: a possible first line of defense. *FEMS Microbiol. Ecol.* **67**, 371–380 (2009).
14. Galloway, S. B. *et al. Coral Disease and Health Workshop: Coral Histopathology II*. (NOAA Technical Memorandum NOS NCCOS 56 and NOAA Technical Memorandum CRCP 4, National Oceanic and Atmospheric Administration, Silver spring, 2007).
15. Peixoto, R. S., Rosado, P. M., Leite, D. C. de A., Rosado, A. S. & Bourne, D. G. Beneficial Microorganisms for Corals (BMC): Proposed Mechanisms for Coral Health and Resilience. *Front. Microbiol.* **8**, (2017).
16. Yang, S.-H. *et al.* Long-Term Survey Is Necessary to Reveal Various Shifts of Microbial Composition in Corals. *Front. Microbiol.* **8**, (2017).
17. Prazeres, M., Ainsworth, T., Roberts, T. E., Pandolfi, J. M. & Leggat, W. Symbiosis and microbiome flexibility in calcifying benthic foraminifera of the Great Barrier Reef. *Microbiome* **5**, 38 (2017).

18. Shiu, J.-H. *et al.* A Newly Designed Primer Revealed High Phylogenetic Diversity of Endozoicomonas in Coral Reefs. *Microbes Environ.* **33**, 172–185 (2018).

19. Hernandez-Agreda, A., Leggat, W., Bongaerts, P., Herrera, C. & Ainsworth, T. D. Rethinking the Coral Microbiome: Simplicity Exists within a Diverse Microbial Biosphere. *mBio* **9**, e00812-18 (2018).

20. Pollock, F. J. *et al.* Coral-associated bacteria demonstrate phylosymbiosis and cophylogeny. *Nat. Commun.* **9**, 4921 (2018).

21. Knowlton, N. & Rohwer, F. Multispecies Microbial Mutualisms on Coral Reefs: The Host as a Habitat. *Am. Nat.* **162**, S51–S62 (2003).

22. Ritchie, K. B. & Smith, G. W. Microbial Communities of Coral Surface Mucopolysaccharide Layers. in *Coral Health and Disease* (eds. Rosenberg, P. E. & Loya, P. Y.) 259–264 (Springer Berlin Heidelberg, 2004).

23. Bourne, D. G. & Munn, C. B. Diversity of bacteria associated with the coral Pocillopora damicornis from the Great Barrier Reef. *Environ. Microbiol.* **7**, 1162–1174 (2005).

24. Koren, O. & Rosenberg, E. Bacteria Associated with Mucus and Tissues of the Coral Oculina patagonica in Summer and Winter. *Appl. Environ. Microbiol.* **72**, 5254–5259 (2006).

25. Johnston, I. S. & Rohwer, F. Microbial landscapes on the outer tissue surfaces of the reef-building coral Porites compressa. *Coral Reefs* **26**, 375–383 (2007).

26. Chiu, H.-H., Mette, A., Shiu, J.-H. & Tang, S.-L. Bacterial Distribution in the Epidermis and Mucus of the Coral Euphyllia glabrescens by CARD-FISH. *Zool. Stud.* 11 (2012).

27. Ainsworth, T. D. *et al.* The coral core microbiome identifies rare bacterial taxa as ubiquitous endosymbionts. *ISME J.* **9**, 2261–2274 (2015).

28. Yang, S.-H. *et al.* Prevalence of potential nitrogen-fixing, green sulfur bacteria in the skeleton of reef-building coral Isopora palifera. *Limnol. Oceanogr.* **61**, 1078–1086 (2016).

29. Glasl, B., Herndl, G. J. & Frade, P. R. The microbiome of coral surface mucus has a key role in mediating holobiont health and survival upon disturbance. *ISME J.* **10**, 2280–2292 (2016).

30. Ainsworth, T. D., Fine, M., Roff, G. & Hoegh-Guldberg, O. Bacteria are not the primary cause of bleaching in the Mediterranean coral Oculina patagonica. *ISME J.* **2**, 67–73 (2007).
31. Work, T. & Aeby, G. Microbial aggregates within tissues infect a diversity of corals throughout the Indo-Pacific. *Mar. Ecol. Prog. Ser.* **500**, 1–9 (2014).
32. Peters, E., Oprandy, J. & Yevich, P. Possible causal agent of" white band disease" in Caribbean acroporid corals. *J. Invertebr. Pathol.* **396**, 394–396 (1983).
33. Peters, E. A survey of cellular reactions to environmental stress and disease in Caribbean scleractinian corals. *Helgol Meeresunters* **137**, 113–137 (1984).
34. Ainsworth, T. & Hoegh-Guldberg, O. Bacterial communities closely associated with coral tissues vary under experimental and natural reef conditions and thermal stress. *Aquat. Biol.* **4**, 289–296 (2009).
35. Neave, M. J. *et al.* Differential specificity between closely related corals and abundant Endozoicomonas endosymbionts across global scales. *ISME J.* (2016). doi:10.1038/ismej.2016.95
36. Work, T. M. & Aeby, G. S. Pathology of tissue loss (white syndrome) in Acropora sp. corals from the Central Pacific. *J. Invertebr. Pathol.* **107**, 127–31 (2011).
37. Wada, N. *et al. In situ* visualization of bacterial populations in coral tissues: pitfalls and solutions. *PeerJ* **4**, e2424 (2016).
38. Wilson, A. C. C. & Duncan, R. P. Signatures of host/symbiont genome coevolution in insect nutritional endosymbioses. *Proc. Natl. Acad. Sci.* **112**, 10255–10261 (2015).
39. Kohl, K. D. & Carey, H. V. A place for host–microbe symbiosis in the comparative physiologist's toolbox. *J. Exp. Biol.* **219**, 3496–3504 (2016).
40. Petersen, J. M. *et al.* Chemosynthetic symbionts of marine invertebrate animals are capable of nitrogen fixation. *Nat. Microbiol.* **2**, 16195 (2017).
41. Yellowlees, D., Rees, T. A. V. & Leggat, W. Metabolic interactions between algal symbionts and invertebrate hosts. *Plant Cell Environ.* **31**, 679–694 (2008).
42. Petrou, K., Nielsen, D. A. & Heraud, P. Single-Cell Biomolecular Analysis of Coral Algal Symbionts Reveals Opposing Metabolic Responses to Heat Stress and Expulsion. *Front. Mar. Sci.* **5**, (2018).

43. Tada, K., Sakai, K., Nakano, Y., Takemura, A. & Montani, S. Size-fractionated phytoplankton biomass in coral reef waters off Sesoko Island, Okinawa, Japan. *J. Plankton Res.* **25**, 991–997 (2003).
44. Tanaka, Y. Nutrient uptake by reef building corals and the ecophysiological effects. *Oceanogr. Jpn.* 101-117 (in Japanese) (2012).
45. Brodie, J. E., Devlin, M., Haynes, D. & Waterhouse, J. Assessment of the eutrophication status of the Great Barrier Reef lagoon (Australia). *Biogeochemistry* **106**, 281–302 (2011).
46. Berkelmans, R., Weeks, S. J. & Steinberga, C. R. Upwelling linked to warm summers and bleaching on the Great Barrier Reef. *Limnol. Oceanogr.* **55**, 2634–2644 (2010).
47. Bourne, D., Iida, Y., Uthicke, S. & Smith-Keune, C. Changes in coral-associated microbial communities during a bleaching event. *ISME J.* **2**, 350–363 (2007).
48. Dinsdale, E. a *et al.* Microbial ecology of four coral atolls in the Northern Line Islands. *PloS One* **3**, e1584–e1584 (2008).
49. Vega Thurber, R. L. *et al.* Metagenomic analysis of stressed coral holobionts. *Environ. Microbiol.* **11**, 2148–2163 (2009).
50. Littman, R., Willis, B. L. & Bourne, D. G. Metagenomic analysis of the coral holobiont during a natural bleaching event on the Great Barrier Reef. *Environ. Microbiol. Rep.* **3**, 651–660 (2011).
51. Kelly, L. W. *et al.* Local genomic adaptation of coral reef-associated microbiomes to gradients of natural variability and anthropogenic stressors. *Proc. Natl. Acad. Sci.* **111**, 10227–10232 (2014).
52. Shiu, J.-H. *et al.* Dynamics of coral-associated bacterial communities acclimated to temperature stress based on recent thermal history. *Sci. Rep.* **7**, 14933 (2017).
53. Glasl, B., Webster, N. S. & Bourne, D. G. Microbial indicators as a diagnostic tool for assessing water quality and climate stress in coral reef ecosystems. *Mar. Biol.* **164**, 91 (2017).
54. Garren, M. & Azam, F. New Method for Counting Bacteria Associated with Coral Mucus. *Appl. Environ. Microbiol.* **76**, 6128–6128 (2010).

55. Garren, M. & Azam, F. Corals shed bacteria as a potential mechanism of resilience to organic matter enrichment. *ISME J.* **6**, 1159–1165 (2012).
56. Sudek, M., Work, T. M., Aeby, G. S. & Davy, S. K. Histological observations in the Hawaiian reef coral, Porites compressa, affected by Porites bleaching with tissue loss. *J. Invertebr. Pathol.* **111**, 121–125 (2012).
57. Bayer, T. *et al.* The Microbiome of the Red Sea Coral Stylophora pistillata Is Dominated by Tissue-Associated Endozoicomonas Bacteria. *Appl. Environ. Microbiol.* **79**, 4759–4762 (2013).
58. van Teeseling, M. C. F., de Pedro, M. A. & Cava, F. Determinants of Bacterial Morphology: From Fundamentals to Possibilities for Antimicrobial Targeting. *Front. Microbiol.* **8**, (2017).
59. Amann, R. I., Ludwig, W. & Schleifer, K. H. Phylogenetic identification and in situ detection of individual microbial cells without cultivation. *Microbiol Mol Biol Rev* **59**, 143–169 (1995).
60. Wagner, M., Horn, M. & Daims, H. Fluorescence in situ hybridisation for the identification and characterisation of prokaryotes. *Curr. Opin. Microbiol.* **6**, 302–309 (2003).
61. Bouvier, T. & del Giorgio, P. A. Factors influencing the detection of bacterial cells using fluorescence in situ hybridization (FISH): A quantitative review of published reports. *FEMS Microbiol. Ecol.* **44**, 3–15 (2003).
62. Prophet, E. B. *Laboratory methods in histotechnology*. (Amer Registry of Pathology, 1992).
63. Riou, V., Périot, M. & Biegala, I. C. Specificity Re-evaluation of Oligonucleotide Probes for the Detection of Marine Picoplankton by Tyramide Signal Amplification-Fluorescent In Situ Hybridization. *Front. Microbiol.* **8**, (2017).
64. Siboni, N., Ben-Dov, E., Sivan, A. & Kushmaro, A. Global distribution and diversity of coral-associated Archaea and their possible role in the coral holobiont nitrogen cycle. *Environ. Microbiol.* **10**, 2979–2990 (2008).
65. Arp, D. J. & Bottomley, P. J. Nitrifers: more than 100 years from isolation to genome sequences. *Microbe-Am. Soc. Microbiol.* **1**, 229 (2006).
66. Feng, G., Sun, W., Zhang, F., Karthik, L. & Li, Z. Inhabitancy of active Nitrosopumilus-like ammonia-oxidizing archaea and Nitrospira nitrite-oxidizing bacteria in the sponge Theonella swinhoei. *Sci. Rep.* **6**, 24966 (2016).

67. Wallner, G., Amann, R. & Beisker, W. Optimizing fluorescent in situ hybridization with rRNA-targeted oligonucleotide probes for flow cytometric identification of microorganisms. *Cytometry* **14**, 136–43 (1993).

68. Daims, H., Brühl, A., Amann, R., Schleifer, K. H. & Wagner, M. The domain-specific probe EUB338 is insufficient for the detection of all Bacteria: development and evaluation of a more comprehensive probe set. *Syst. Appl. Microbiol.* **22**, 434–44 (1999).

69. R Core Team. R: A Language and Environment for Statistical Computing. *Vienna, Austria: R Foundations for Statistical Computing.* (2013).

70. Signorell, A. DescTools: Tools for descriptive statistics (R package version 0.99.26). *The Comprehensive R Archive Network* (2018).

71. Wickham, H., François, R., Henry, L., Müller, K. & RStudio. dplyr: a grammar of data manipulation (R package version 0.7.6). *The Comprehensive R Archive Network* (2018).

72. Ogle, D., Wheeler, P. & Dinno, A. FSA: Simple Fisheries Stock Assessment Methods (R package version 0.8.20). *The Comprehensive R Archive Network* (2018).

73. Sarkar, D. *Lattice: multivariate data visualization with R.* (Springer Science & Business Media, 2008).

74. Mangiafico, S. rcompanion: Functions to Support Extension Education Program Evaluation (R package version 2.0.0). *The Comprehensive R Archive Network* (2018).

Figure legends

Fig. 1 Map showing the locations of five study sites in two countries: **(a, b)** Sesoko Island (SI) in Okinawa, Japan; **(a, c)** Inner Shelf (IS), Lizard Island (LI) and Outer Shelf

(OS) sites in the Northern Great Barrier Reef; and **(a, d)** Orpheus Island (OI) in the central Great Barrier Reef, Australia.

Fig. 2 Histological appearance, occurrence and density of CAMAs in the coral *Acropora hyacinthus.* (**a**) Numerous CAMAs (indicated by arrows) are visible in a histological section stained by hematoxylin and eosin of a colony from Sesoko, Japan. (**b**) Right panel shows close-up of a CAMA located in a mesentery of a polyp from the branch sectioned in (a). **(c)** Pie diagrams showing the proportion of colonies sampled that contained CAMAs at five sites in Japan and Australia. A significantly higher proportion of Sesoko Is. samples contained CAMAs than samples collected from three more offshore sites (Lizard Is., Outer Shelf northern GBR site, and Orpheus Is.) (**p<.005; G test followed by a post-hoc bonferroni). **(d)** Densities of basophilic-staining (upper graph) or eosinophilic-staining (lower graph) CAMAs at five sites. Densities of basophilic CAMAs were significantly greater in samples from Sesoko Is. than in samples from the three offshore sites (Lizard Is., Outer Shelf site, and Orpheus Is, as were densities in the Inner shelf GBR site compared to the two offshore northern sector sites (** p<005; Kruskal-Wallis test, with Dunn's multiple comparison followed by a bonferroni correction). Scale bars indicate 600 µm (**a**), 50 µm (**b**) and 10 µm **(d)**.

Fig. 3 Distribution of CAMAs within six anatomical regions of the coral *Acropora hyacinthus* collected from five sites in Japan and Australia. (a) Schematic drawing of a coral polyp showing the six anatomical regions examined microscopically (same colour coding used in b) and c)). **b)** Pie charts showing the distribution of CAMAs among six anatomical regions in samples from the five sites. **(c)** Dot plots comparing the size of CAMAs among anatomical regions for each location. N=307 CAMAs detected in tissues treated with FISH.

Fig. 4 Morphological variation in bacteria housed within different CAMAs. Note that bacteria within each CAMA are morphologically similar. Dotted lines (in **a**–**d** and **i**–**l**) delineate regions magnified in close-up images (**e**–**h** and **m**–**p**). Overall, five bacterial morphologies were detected: rod-like (**a**, **e**), pleomorphic (**b**, **f**), long rods (**c**, **g**), filamentous-like (**d**, **h**), rod-shaped with spore-like structures (**i**–**j** and **m**–**n**), and putative amorphous masses (k–l and o–p). Scale bars indicate 10 µm (**a**–**d** and **i**–**l**) and 5 µm (**e**–**h** and **m**–**p**).

Fig. 5 Three-dimensional (3D) images of CAMAs (red) within a tentacle of the coral *Acropora hyacinthus*, as visualized using FISH. (**a)** Section of tentacle showing localization of two types of CAMAs (10x magnification). **(b)** Single aggregation of bacteria in a large structure within the ectoderm (40x magnification; composed of 92 z-stack images). **(c)** Multiple aggregations of bacteria in smaller structures within the

gastrodermis (40x magnification; composed of 56 z-stack images). 3D rendering of CAMAs (**d** and **e**) reconstructed from 3D images in **b** and **c**. Coral tissue and *Symbiodiniaceae* appear as blue and green structures, respectively.

Suppl. Fig. 1 Calculating the area of CAMAs. **(a)** A single large CAMA, comprised of rod-shaped bacteria, was calculated to be 175.7 μm^2 in cross-sectional area from 3D images. **(b)** Smaller, numerous aggregations were calculated to be, on average, 22.6±4.2 μm^2 in cross-sectional area (n = 8). Scale bars indicate 20 µm.

Suppl. Fig. 2 Schematic drawing showing how coral fragments were sectioned for H&E staining and FISH. In total, nine sections were collected from each sample (three sets of sections, each set comprised of three serial sections). *1: Distance between each set was 100 µm.

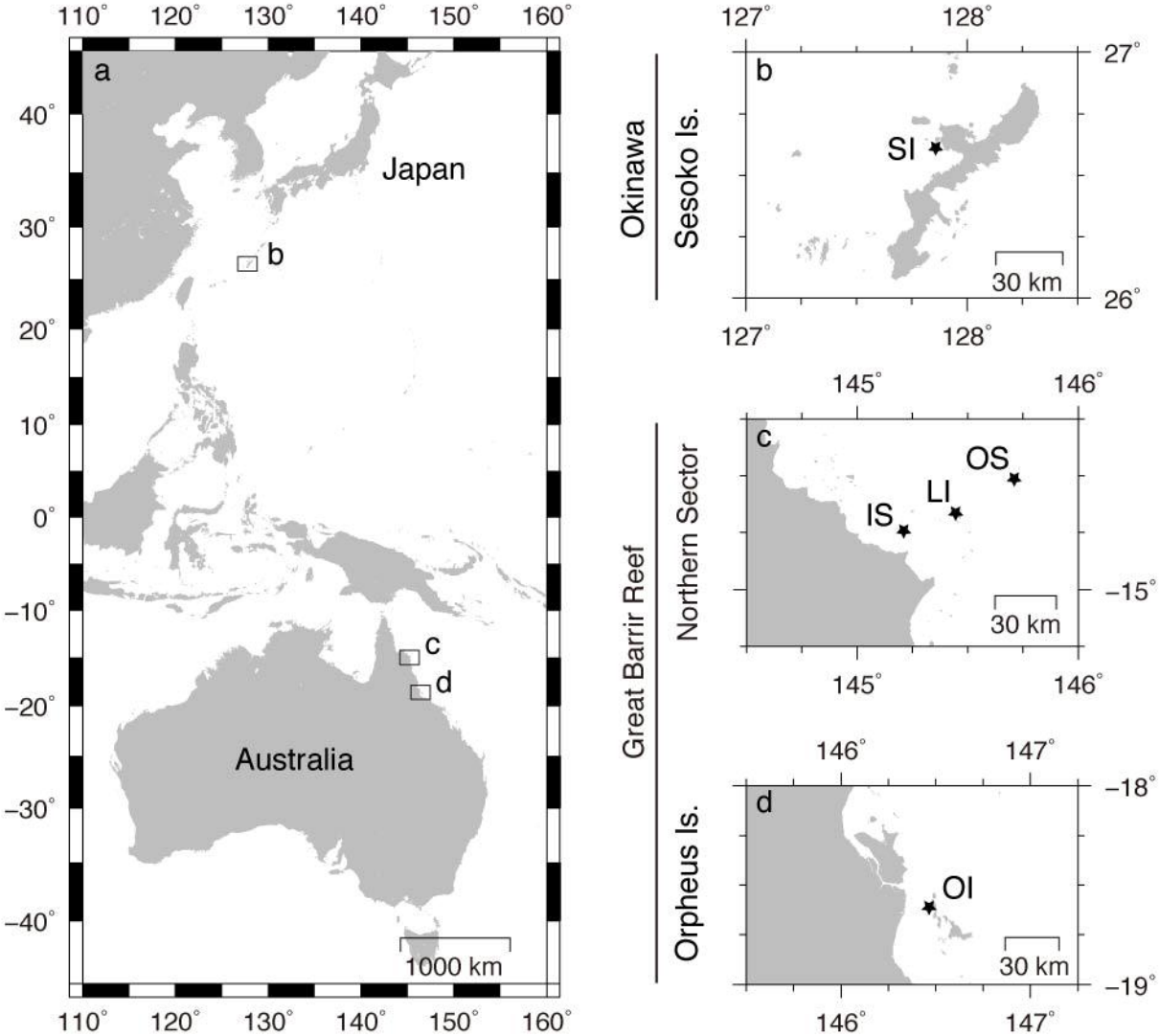
a
Japan
b
c
d
Australia
1000 km
110°
120°
130°
140°
150°
160°
40°
30°
20°
10°
0°
−10°
−20°
−30°
−40°
Okinawa
Sesoko Is.
SI
30 km
127°
128°
27°
26°
Great Barrir Reef
Northern Sector
OS
LI
IS
145°
146°
−15°
Orpheus Is.
OI
147°
−18°
−19°

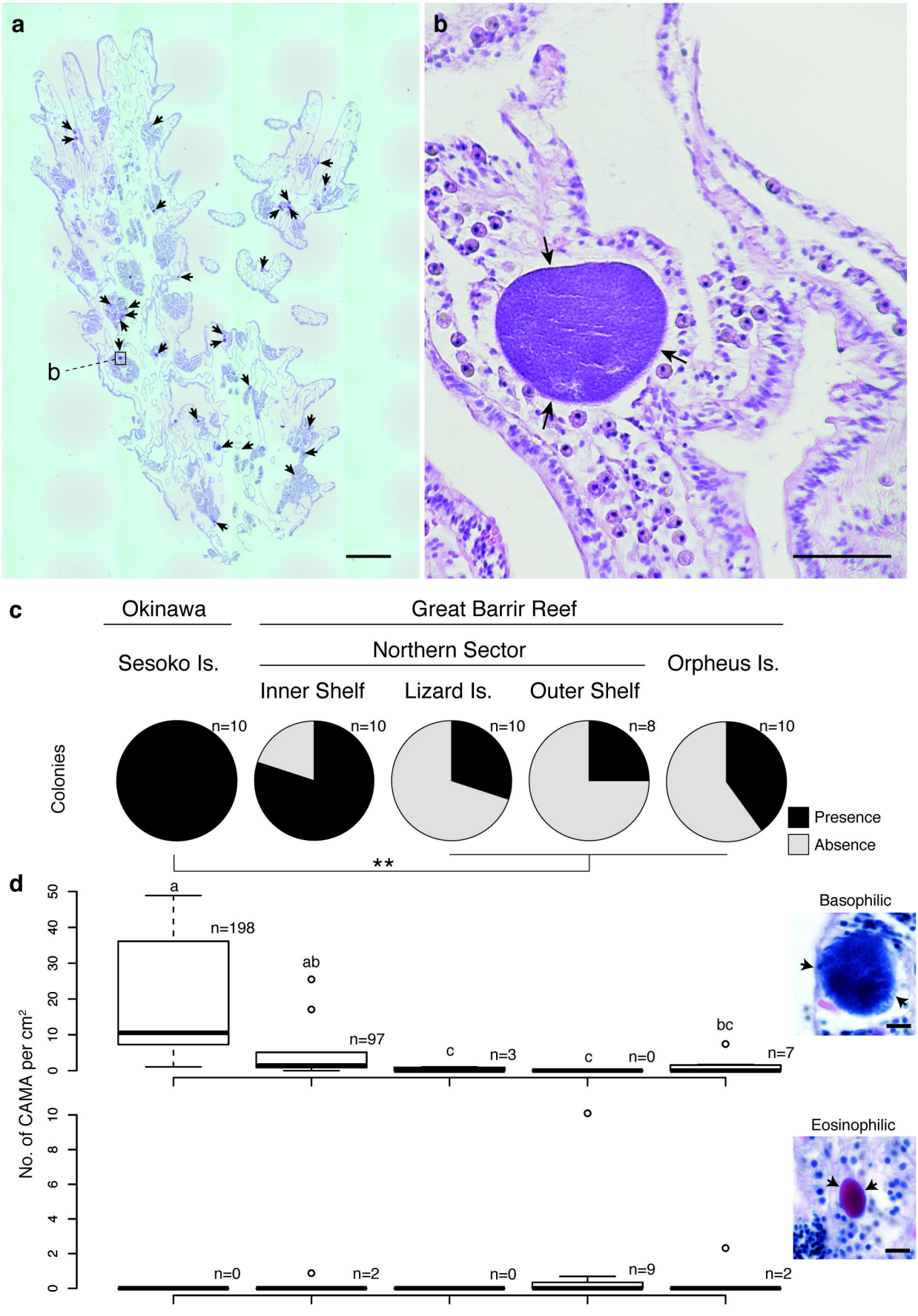
a
b
b
c
Okinawa
Great Barrir Reef
Sesoko Is.
Northern Sector
Orpheus Is.
Inner Shelf
Lizard Is.
Outer Shelf
Colonies
n=10
n=10
n=10
n=8
n=10
Presence
Absence
**
d
No. of CAMA per cm²
a
n=198
ab
n=97
c
n=3
c
n=0
bc
n=7
Basophilic
n=0
n=2
n=0
n=9
n=2
Eosinophilic

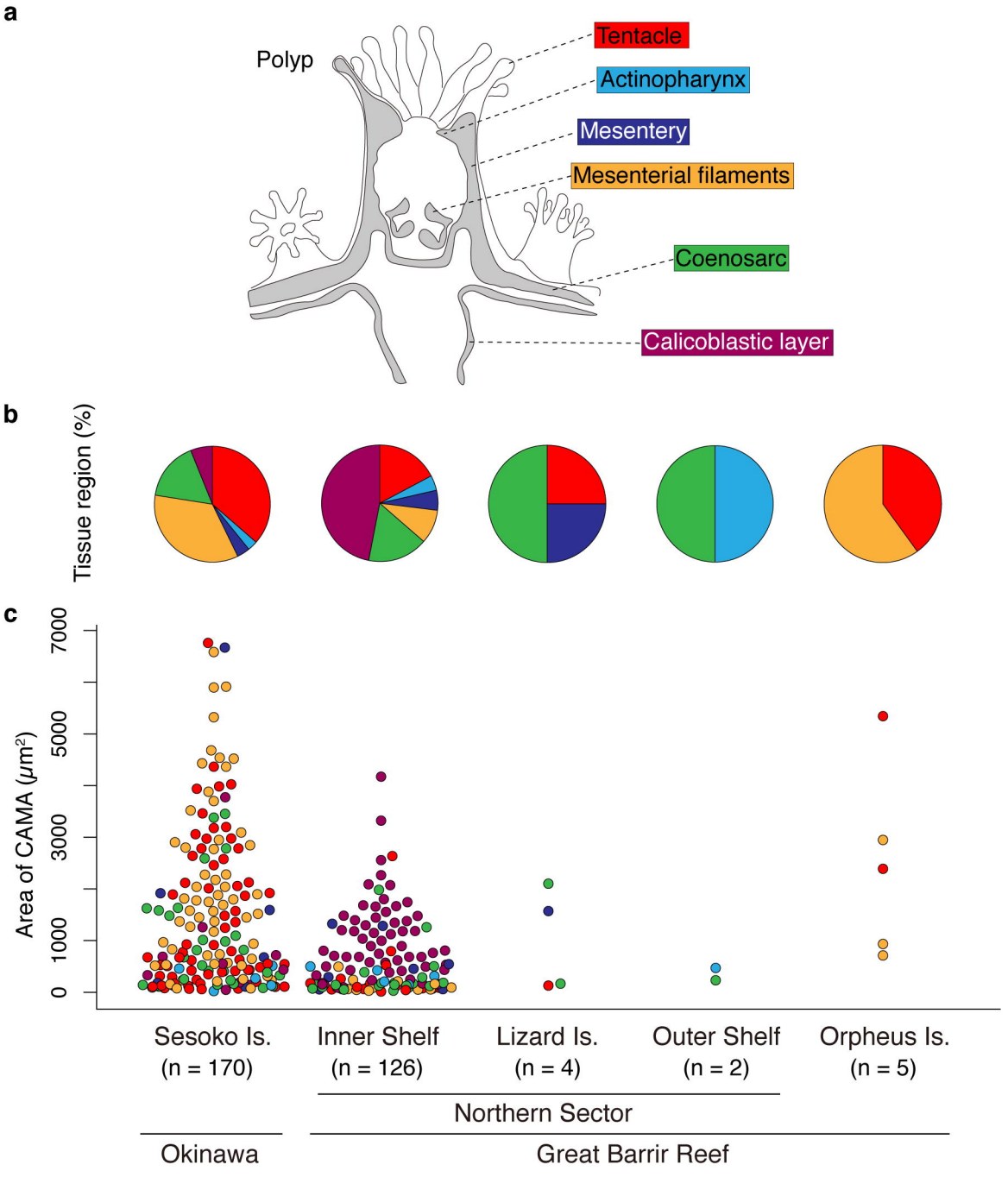
a
Polyp
Tentacle
Actinopharynx
Mesentery
Mesenterial filaments
Coenosarc
Calicoblastic layer
b
Tissue region (%)
c
Area of CAMA (μm²)
0
1000
3000
5000
7000
Sesoko Is.
(n = 170)
Inner Shelf
(n = 126)
Lizard Is.
(n = 4)
Outer Shelf
(n = 2)
Orpheus Is.
(n = 5)
Northern Sector
Okinawa
Great Barrir Reef

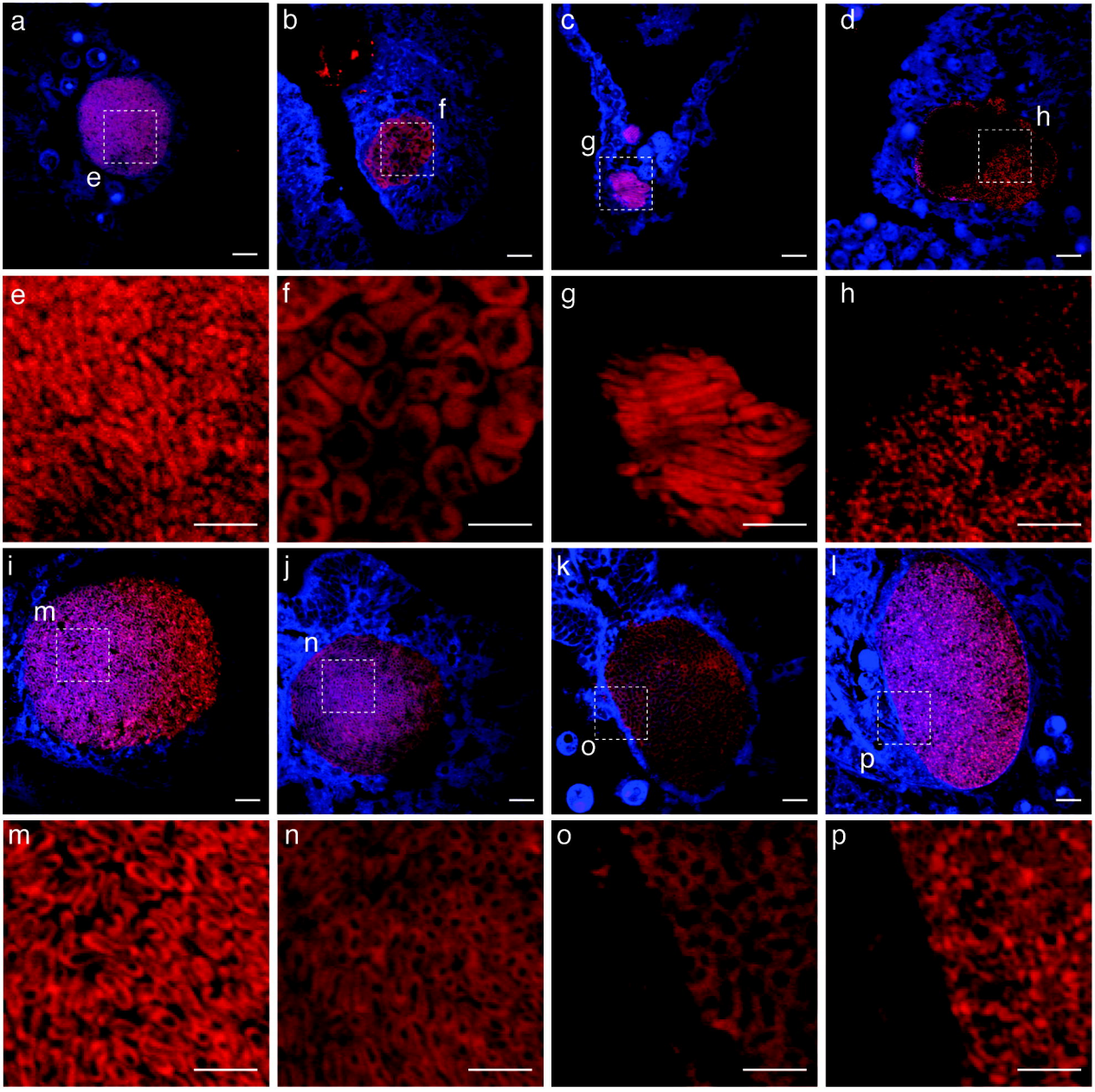
a
b
c
d
e
f
g
h
i
j
k
l
m
n
o
p

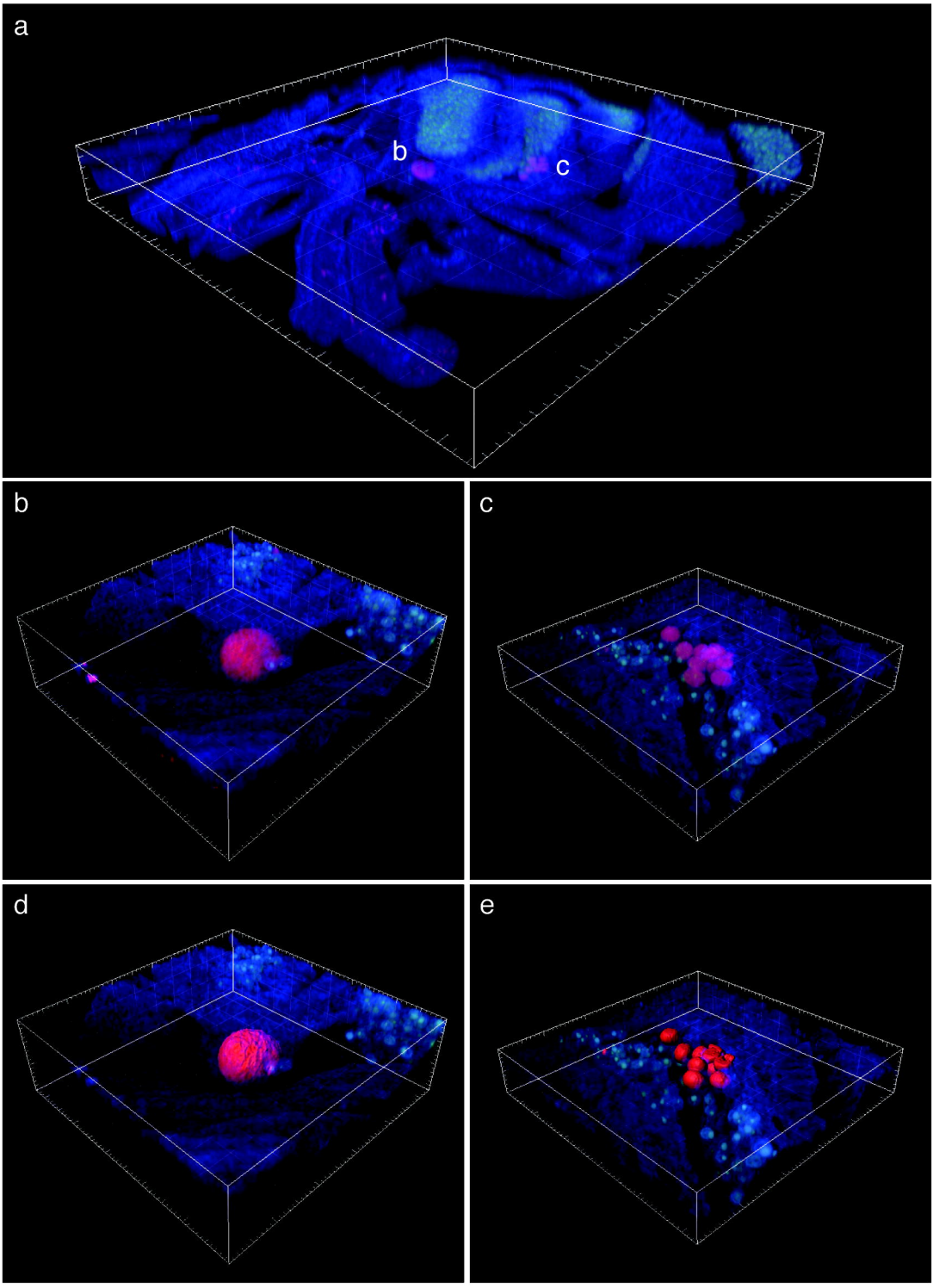
a
b
c
b
c
d
e